Check for updates

MR. ARTURO OTTAVIO RINALDI (Orcid ID : 0000-0001-8967-3866)
DR. GE TAN (Orcid ID : 0000-0003-0026-8739)
DR. PETER SCHMID-GRENDELMEIER (Orcid ID : 0000-0003-3215-3370)
PROF. CEZMI AKDIS (Orcid ID : 0000-0001-8020-019X)

Article type : Original Article: Atopic Dermatitis, Urticaria and Skin Disease

Manuscript Acceptance Date: 23-Mar-2021

Electrical impedance spectroscopy for the characterization of skin barrier in atopic dermatitis

Short title**:** A new tool for skin barrier assessment in AD

Arturo O. Rinaldi[1,], Angelica Korsfeldt[2], Siobhan Ward[1,3], Daniel Burla[1], Anita Dreher[3], Marja Gautschi[4], Britta Stolpe[4], Ge Tan[1,5], Eugen Bersuch[3], David Melin[2], Nima Askary Lord[2], Simon Grant[2], Per Svedenhag[2], Kristina Tsekova[4], Peter Schmid-Grendelmeier[3,6], Matthias Möhrenschlager[4], Ellen D. Renner[4,7], Cezmi A. Akdis[1,3*]

Affiliations

1 Swiss Institute of Allergy and Asthma Research (SIAF), Davos, Switzerland

2 SciBase AB, Sundbyberg, Sweden

3 Christine Kühne – Center for Allergy Research and Education (CK-CARE), Davos, Switzerland

4 Hochgebirgsklinik - High Altitude Clinic (HGK), Davos, Switzerland

5 FunctionalGenomics Center Zurich, ETH Zurich/University ofZurich, Zurich, Switzerland

6 Department of Dermatology, University Hospital, Zurich

This article has been accepted for publication and undergone full peer review but has not been through the copyediting, typesetting, pagination and proofreading process, which may lead to differences between this version and the Version of Record. Please cite this article as doi: 10.1111/ALL.14842

This article is protected by copyright. All rights reserved

Accepted Article

7 Environmental Medicine - UNIKA-T, Technical University, Munich and Helmholtz Center

Corresponding author

Cezmi A. Akdis, Swiss Institute of Allergy and Asthma Research (SIAF), Herman Burchard Strasse 9, CH-7265, Davos, Tel +41814100841, Email akdisac@siaf.uzh.ch

Accepted Article

This article is protected by copyright. All rights reserved

Acknowledgments

We acknowledge the contribution of Ass. Professor StigOllmar (founder of SciBase) for his basic research within this area. We also thank Beate Rückert and Anja Heider for their technical assistance during the study and Anna Głobińska for her help with the graphical abstract. **Funding**: This study was funded by the Swiss National Foundation and the Christine Kühne Center for Allergy Research and Education. SciBase AB contributed EIS instruments and electrodes for the study and contributed towards study funding. **Author contributions**: Rinaldi AO, Ward S and Burla Dperformed patient measurements. Dreher A, Gautschi M, Stolpe B, Tsekova K, Möhrenschlager M and Renner E provided clinical and data collection assistance. Tan G and Rinaldi AO performed genome data analyses. Korsfeldt Aand SciBasedeveloped the artificial intelligence (EIS) algorithms. Rinaldi AO performed and had overall responsibility for data analysis. All authors contributed to data analysis and the writing and review of this article. **Competing interests**: Korsfeldt A, Melin D, Askary N, Grant S and Svedenhag P are employees of SciBase AB. Akdis CA, Rinaldi AO and Grant S are co-inventors PCT Patent application WO2020094357A1 entitled 'Methods and medical devices for analyzing epithelial barrier function'.

Conflict of interest

AR, **SG** and **CA** report a pending patent application on "Methods and medical devices for analyzing epithelial barrier function". **AK**, **DM**, **AL**, **SG**, **PS** declare receiving personal fees from SciBase AB. **CA** reports grants from Allergopharma, Idorsia, Swiss National Science Foundation, Christine Kühne-Center for Allergy Research and Education, European Commission Horizon 2020 Framework Programme, Cure, Novartis Research Institutes, Astra Zeneca, SciBase, and is on the Sanofi/Regeneron advisory board. **WS**, **DB**, **AD**, **MG**, **BS**, **GT**, **EB**, **KT**, **PS-G**, **MM** and **ER** have nothing to declare within the scope of this work.

This article is protected by copyright. All rights reserved

Accepted Article

Abbreviations

AD: Atopic dermatitis

Adjacent: An area of the body which is visually unaffected but is close to a lesional area

BIRC2: Baculoviral IAP Repeat Containing

CCL: C-C motif chemokine ligand

CDSN: Corneodesmosin

CXCL: C-X-C motif chemokine ligand

EIS algorithm: Artificial intelligence model based on EIS measurements

EIS score: The score given to a measurement by the EIS algorithms.

EIS: Electrical impedance spectroscopy

FG2: Fibroblast growth factor 2

FLG: Filaggrin

IRAK: Interleukin 1 Receptor Associated Kinase

PATJ: Protein associated to tight junctions

SCORAD: Scoring atopic dermatitis

TEWL: Transepidermal water loss

TJs: Tight junctions

TNFSF14: Tumor necrosis factor superfamily 14

Accepted Article

This article is protected by copyright. All rights reserved

Abstract

Background: Allergic disorders such as atopic dermatitis (AD) are strongly associated with an impairment of the epithelial barrier, in which tight junctions and/or filaggrin expression can be defective. Skin barrier assessment shows potential to be clinically useful for prediction of disease development, improved and earlier diagnosis, lesion follow-up and therapy evaluation. This study aimed to establish a method to directly assess the *in vivo* status of epithelial barrier using electrical impedance spectroscopy (EIS).

Methods: 36patients with AD were followed during their 3-week hospitalizationand compared with 28 controls. EIS and transepidermal water loss (TEWL) were measured in lesional and non-lesional skin. Targeted proteomics by proximity extension assay in serum and whole-genome sequence were performed.

Results: EIS was able to assess epithelial barrier integrity, differentiate between patients and controls without AD and characterize lesional and non-lesional skin of patients. It showed a significant negative correlation with TEWL, but a higher sensitivity to discriminate non-lesional atopic skin from controls. During hospitalization, lesions reported a significant increase in EIS that correlated with healing, decreased SCORAD and itch scores. Additionally, EIS showed a significant inverse correlation with serumbiomarkersassociated with inflammatory pathways that may affect the epithelial barrier,particularly chemokines such as CCL13, CCL3, CCL7, CXCL8, and other cytokines, such as IRAK1, IRAK4 and FG2, which were significantly highat admission.Furthermore, filaggrin copy numbers significantly correlated with EIS on non-lesional skin of patients.

Conclusions: EIS can be a useful tool to detect skin barrier dysfunction *in vivo*, valuable for the assessment of AD severity, progression and therapy efficacy.

Keywords

Atopic dermatitis; electrical impedance spectroscopy;epithelial barrier; skin barrier assessment; biomarkers.

This article is protected by copyright. All rights reserved

Accepted Article

Accepted Article

This article is protected by copyright. All rights reserved

Accepted Article

Introduction

Atopic dermatitis (AD) is a chronic relapsing inflammatory skin disorder characterized by pruritus, excoriations, dry skin and susceptibility for cutaneous infections. It is one of the most common skin diseases, affecting up to 20% of children and 3% of adults worldwide.[1, 2] It has detrimental effects on the quality of life of patients and their families and represents a high socioeconomic burden.[3]Dysfunction of the epidermal barrier seems to play a crucial role in the complex and multifactorial pathophysiology of AD, leading to an increased penetration of allergens into the skin and resulting in increased allergic sensitization.[4] Defects in the epidermal barrier can be caused by environmental risk factors and be the result of a genetic predisposition as well as *S. aureus* colonization.[5] Mutations and polymorphisms of skin barrier-related genes have been identified in patients with AD in the past decades. In particular, mutations of filaggrin (*FLG*), which has a pivotal role in the formation of the cornified envelope in the stratum corneum, are frequent in patients with severe AD.[6] In addition, the human *FLG* gene is polymorphic with an intragenic copy number variation. Specifically, 10, 11, or 12 nearly identical tandem repeats can be present in the exon 3. Each repeat encodes a complete polypeptide, therefore the intragenic copy number variation can affect the number and quantity of filaggrin molecules expressed in the epidermis. Low copy numbers of filaggrin are associated with higher AD risk.[7] Furthermore, polymorphic variants of genes coding for tight junction (TJ) proteins are expressed in stratum granulosum. The contribution of TJs to skin barrier function is fundamental and has been significantly associated with AD.[8]

The diagnosis of AD relies on the morphology and the distribution of skin lesions, as well as on associated features of the patient, such as pruritus, atopy or familial predisposition to atopic disease.[2] The diagnosis remains clinical, since no reliable biomarkers can uniquely distinguish the disease from others.[9, 10] AD is highly heterogeneous and has been divided into clinical phenotypes based on age of onset, severity, and history of bacterial or viral infections.[11, 12] Therefore, biomarkers for the stratification of patients, the prediction of a treatment response and the monitoring of AD severity would be of great added value, offering more reliable and objective outcome measures. In addition, recent studies have shown that barrier integrity measurement in infants shows potential as an early biomarker to predict the development of both AD and food allergies.[13, 14] This in turn may help lead to the development of preventive approaches and

This article is protected by copyright. All rights reserved

decrease the disease burden.[15, 16] Furthermore, the impact of skin barrier on the pathophysiology of AD has been largely described, however so far methods to evaluate it *in vivo* are lacking or restricted to a research setting.[17, 18] Recently, in several mouse models of skin barrier dysfunction, our group described electrical impedance spectroscopy (EIS) as an efficient tool to detect skin barrier defects caused by various enzymes such as papain, trypsin, cholera toxin, as well as by tape-stripping.[19] By measuring the electrical impedance across wide frequency ranges and depths, electrical resistance information in the tissues regarding both intra and extracellular tissue properties can be collected. The EIS method is relatively quick and robust and does not appear to suffer from the limitations seen in other methods, such as Trans Epidermal Water Loss (TEWL) or Raman Spectroscopy.[20, 21] In the present study, we demonstrate the ability of EIS to characterize the epidermal barrier function directly in patients with AD, suggesting a broad potential for early diagnosis, evaluation of therapy response and assessment of disease severity. In addition, we correlate the EIS findings with circulating inflammatory protein biomarkers and mutations in skin barrier genes.

Accepted Article

This article is protected by copyright. All rights reserved

Materials and methods

Clinical study description

Thirty-six patients diagnosed with AD were recruited during their hospitalization at the High-Altitude Clinic in Davos, Switzerland. The inclusion criteria for patients in this study were that they be 18-85 years of age and have received a clinical diagnosis of AD.

The inclusion of patients was independent from their current therapy at the time of the recruitment. Throughout their stay at the High-Altitude Clinic in Davos, patients received different types of topical and/or systemic treatments as routine treatment procedures independent from the present study. Twenty-eight controls without AD were investigated in parallel. The inclusion criteria for controls in this study were that they be 18-85 years of age and have never received a clinical diagnosis of AD. Demographics, such as gender ratio, ethnicity and average age are comparable between AD and control groups (Table 1).

Peripheral blood was taken from twenty-nine out of the thirty-six AD patients on their first day of hospitalization and at the end of their third week. In seventeen of the controls peripheral blood was taken, but only once. Ethical permission for the study was obtained from the ethical committee of the Canton of Zurich. Informed consent was obtained after the nature and possible consequences of the study have been explained.

Clinical data collection

Patients were assessed throughout their stay at the High-Altitude Clinic Davos at three different time points (visits 1-3). For each of the time points, dermatologists calculated SCORAD (Scoring Atopic Dermatitis) according to the official guidelines.

EIS measurements

EIS measurements were made using Nevisense® (SciBase, Sweden), a device and single use electrode established for skin cancer detection and general research. EIS is the measure of a material's opposition to the flow of alternating currents at various frequencies. Specifically, tissue EIS can reflect the pathophysiological status of the tissue. Normal and abnormal tissue may differ with regards to cell size, shape, orientation, compactness and structure of cell membranes. The

This article is protected by copyright. All rights reserved

system measures the electrical impedance at 35 different frequencies distributed between 1 kHz and 2.5 MHz at four depths in 10 permutations, resulting in 700 data points per measurement. The applied voltage and current are limited to 150 mV and 75 μA, respectively, and are imperceptible to the patient. The broad frequency range allows collection of information on both intra- and extracellular tissue properties. Nevisense is equipped with a handpiece and a disposable 5 mm by 5 mm electrode. A single Nevisense impedance measurement takes less than a minute and consists of first moistening the skin with physiological saline solution, then applying the electrode to the area to be examined for the 8 second measurement.

For each patient involved in the study, EIS measurements were performed on a lesion, on a non-lesional area adjacent to the lesion and on the volar forearm two centimeters from the antecubital region. In particular, among the patients included in the present study:

- 15 patients had the lesion on the dorsal forearm,
- 16 patients had the lesion on a body site different than forearm (neck, hands, forehead),
- 5 patients had no lesion at the time of the measurements.

The volar forearm, measured in all patients, was non-lesional in 19 patients and lesional in the remaining 17 patients at the time of the recruitment.

Measurements were performed on the same body sites in controls and in AD patients. All measurements were done in triplicates in both patients and controls.

Development of neural network algorithms

The aim was to develop the following potentially useful EIS-based clinical algorithms:

- to differentiate between subjects with AD and healthy subjects based on a measurement on (visually) unaffected skin
- to assess lesions and the extent of subclinical skin barrier damage adjacent to lesions
- to follow up and evaluate lesional areas during healing/restoration process

To achieve this we randomly separated AD patients and healthy controls into two groups: one group for the training of the neural network algorithms and one group for the validation of the algorithms (Supplementary figure 4; full details are included in supplementary material and methods). EIS algorithms based on neural networks were developed using raw EIS measurement data collected from both subjects with AD and healthy subjects.The EIS algorithms use an EIS

This article is protected by copyright. All rights reserved

measurement as input and output a score between 0 and 1. The score represents the likelihood of a defective skin barrier, where 0 represents a defective barrier and1 a healthy barrier.

Significant site-specific variations in the skin barrier have been reported in barrier function measurements and so measurement location must be considered.[22] The forearm has been used as a standard area in previous studies and in our study was the body site where patients most frequently had lesions and therefore where we performed the most measurements. For these reasons, we developed EIS algorithms for the forearm. Specifically, we developed three algorithms and validated them using separate validation data sets (Supplementary table 5):

- **Non-lesional algorithm**; to differentiate between subjects with or without AD based on measurements on the visually non-affected volar forearm (3 cm from the antecubital fossa).
- **Lesional algorithm;** to assess lesional skin and the extent of subclinical barrier damage in visually non-lesional skin adjacent to lesional skin. Measurements on both lesional and non-lesional skin on the dorsal forearm were used. The dorsal forearm was the body site with the most measurements on both lesional skin and non-lesional skin adjacent to the lesion.
- **Follow-up algorithm**; to follow the healing of the lesions and the restoration of skin barrier on the dorsal forearm of AD patients.

In Figure 1, the EIS scores presented are only from the validation data set. In other figures we used EIS scores from both the training and validation data sets, since the training data were not related to these other data types and the purpose of the analysis was to investigate how these data correlate with EIS scores.

TEWL measurements

TEWL was measured by the "Delfin VapoMeter©" (Delfin Technologies, Finland), whose core is a sensitive humidity sensor within a closed chamber. Its sensor monitors the increase of relative humidity inside the chamber during the skin measurement and automatically calculates the evaporation rate value (g/m^2h) from the relative humidity increase. TEWL and EIS measurements were always performed in the same room and at the same body sites.

This article is protected by copyright. All rights reserved

Multiplex proximity extension assay

Peripheral blood was collected and centrifuged, and plasma samples were stored at –80°C until further processing. Aliquots were analyzed by the targeted proteomics (Olink, Uppsala, Sweden) proseek multiplex assay, a proximity extension assay (PEA), using the established 96-plex panels named inflammation and immune response, each spanning 92 proteins. This technology uses oligonucleotide-labeled antibody probe pairs that bind to their respective targets. Only upon binding of both antibody pairs to their target, DNA reporter molecules bound to the antibodies can form a double strand DNA that is amplified and quantified by a real-time polymerase chain reaction assay. Data were obtained as NPX (Normalized Protein eXpression) values, Olink's arbitrary unit which is in Log2 scale. The NPX scale is inverted compared to that of Ct, meaning that a high NPX value equals a high protein concentration.

Pathway analysis was conducted using MetaCore software (Clarivate Analytics). The differentially expressed protein lists with p-value and $\log_2$-fold change were uploaded and the results of the enrichment analysis provided pathway maps, which were determined to be of statistical significance.

Whole-genome sequencing and variant calling

Whole-genome sequencing was performed on patients and controls with Illumina TruSeq DNA Nano Kit. To discover variants, a GATK best practices pipeline was followed.[23] In brief, the next generation sequencing reads were mapped to Ensembl human reference genome GRCh38.p10 release 91 with Bowtie2 v2.3.2, then duplicates were marked and base quality scores were recalibrated.[24, 25] After calling variants per sample, a joint-call of genotyping was performed.

Statistics

Mann-Whitney U test was used to compare differences between two different unrelated groups, such as patients with AD and controls. Wilcoxon test was used to compare differences between paired variables within the same patient, such as lesional and adjacent non-lesional skin. Correlations between EIS scores, proteins in serum and severity scores were evaluated by Spearman's rank test. All the statistical analyses were performed with GraphPad Prism 8.3 (GraphPad Software). A p-value of <0.05 was considered statistically significant.

This article is protected by copyright. All rights reserved

Receiver operating characteristic (ROC) curves were used to analyze the sensitivity and specificity performance of the EIS algorithms and TEWL. The area under the ROC curve (AUC) is a measure of an algorithm ability to separate between two clinical groups and it can be between 0 and 1. The higher the AUC is, the better the algorithm is at differentiating between two groups.

Olink data were imported in Normalized protein expression (NPX) format, processed by "OlinkRPackage" from Olink Proteomics (https://github.com/Olink-Proteomics/OlinkRPackage). The statistical comparison of protein levels between groups was performed with Bioconductor limma package (https://bioconductor.org/packages/limma/). The fold change and p-value were estimated by fitting a linear model for each protein.For multiple testing adjusted p-value was calculated with Benjamini and Hochbergmethod. The results were summarized in a volcano plot, with the magnitude of change in x-axis and the significance level in y-axis.

Accepted Article

This article is protected by copyright. All rights reserved

Results

EIS can differentiate between the skin of healthy subjects and the lesional or non-lesional skin of AD patients

We analyzed the skin of healthy controls and AD patients (Table 1) over a 3 week treatment period, using four different methods (EIS, TEWL, proteomic and genetic analysis). Artificial intelligence-based algorithms were trained to discriminate between the electrical impedance response of AD patients and that of healthy controls and generate an EIS score between 0 and 1. The closer the EIS score is to 1, the higher the correlation is to a stronger barrier and healthier skin. In contrast, the closer the score is to 0, the weaker the skin barrier.

Figure 1A illustrates that the EIS algorithm can differentiate between the skin of healthy controls and the non-lesional skin of AD patients, with limited overlap between the two groups; whereas TEWL measurements from the same two groups show no significant difference. Furthermore, when comparing healthy skin on the dorsal forearm of controls with lesional skin or non-lesional skin adjacent to a lesion of AD patients, we observed significantly different EIS scores between all the three groups. However, TEWL increased in lesional skin, but with relatively low significance and less differentiation between the groups (Figure 1B). The use of emollients prior to the measurements did not appear to affect the overall results but this requires further investigation (Supplementary figure 1). EIS showed promising diagnostic ability with relatively good sensitivity and specificity, as shown in the ROC curves in figure 1C-. In these plots, the closer the area under the curve (AUC) is to 1, the better the algorithm is at differentiating between the two groups. When comparing the respective AUCs, EIS was significantly better than TEWL in separating between the skin of controls and the non-lesional or adjacent skin of AD patients (Figure 1C and Supplementary figure 2A), and in characterizing lesional and adjacent skin (Supplementary figure 2B). Both EIS and TEWL showed almost 100% sensitivity and specificity in separating AD lesions from healthy control skin (Supplementary figure 2C).

Significantly upregulated inflammation- and immune response-related proteins correlate with EIS scores

This article is protected by copyright. All rights reserved

Accepted Article

To characterize the immune status of the AD patients, the expression of inflammation- and immune response-related proteins was analyzed in serum by using the multiplex proximity extension assay. At the time of their hospitalization, AD patients presented significantly higher levels of several proteins compared to the control group (Figure 2A and B). Out of 182 different proteins analyzed,60 showed a significant difference between AD and controls. The most significant 9 proteins are shown in figure 2B and the remainder are listed in supplementary table 1 (Supplementary table 1).

To understand how differentially expressed proteins are linked to biological mechanisms, we performed enrichment analysis with MetaCore software to examine the role of these proteins within molecular pathways. Many of the most significantly enriched pathways (Figure 2C and Supplementary figure 3) were associated with the tissue migration of mast cells, eosinophils, basophils and neutrophils, all of which may have an influence on the epithelial barrier status. Not only did EIS show a significant inverse correlation with many proteins involved in those pathways, such as CCL13, IRAK1, TNFSF14, BIRC2, FGF2, CCL3, CCL7, and CXCL8 (Figure 2D), but it also correlated inversely with many other important proteins involved in other inflammatory and immune-related processes (Figure 2E and Supplementary table 2). In conclusion, data suggest that the more pronounced the inflammatory state of a patient is, the more barrier function appears to be affected. EIS therefore represents a good candidate as a rapid method to evaluate skin inflammation and can be particularly useful in differentiating healthy from skin affected by sub-clinical inflammation.

Lesion healing in response to treatment correlates with an increase in EIS scores and a decrease in TEWL

AD patients were hospitalized for approximately 3 weeks and during this time EIS and TEWL were measured three times. From the admission (visit 1 or first visit) to the end of the treatment (visit 3 or last visit), their lesional skin showed a significant increase in EIS scores and a significant decrease in TEWL (Figure 3A and B), indicating a restoration of the skin barrier integrity probably due to the received treatment, as confirmed by improved SCORAD (Supplementary table 3). EIS scores and TEWL showed a significant inverse correlation: when the former increased, the latter decreased (Figure 3C). Furthermore, in AD patients the lesion improvement assessed by the increase in EIS scores correlated with the reduction of pruritus. In

This article is protected by copyright. All rights reserved

fact, the difference between first and last visit EIS scores showed a strong significant and inverse correlation with the difference of pruritus scores between first and last visit (Figure 3D). In addition, EIS scores calculated on the lesional forearm at both visits showed a significant correlation not only with the pruritus score (Figure 3E), but also with the SCORAD (Figure 3F) calculated at the same visits. These data show a correlation of improvement in EIS scores with clinical healing, confirmed by the improvement in SCORAD and pruritis scores.

The change in EIS score during the 21-day treatment correlates with the correction of proinflammatory proteins in the direction of healthy controls

To investigate protein changes in the AD patients throughout their hospitalization, the expression of inflammation- and immune response-related proteins was analyzed in serum by using the multiplex proximity extension assay both at admission and at discharge. As shown in the volcano plot in figure 4A and in supplementary table 4, treatment significantly affected the serum level of several inflammatory proteins, causing their down- or upregulation. In particular, CCL13 and Corneodesmosin (CDSN), a skin barrier integrity marker altered in patients with skin barrier-related disorders[26], were downregulated by the treatment, whereas CXADR, which has been reported to be essential for tight junction integrity and to be involved in the repair of epithelial tissues [27, 28], was upregulated (Figure 4B). CDSN levels in AD patients decreased to levels similar to those observed in the control group. Interestingly, the difference of EIS scores on the dorsal forearm between first and last visit showed a strong and significant inverse correlation with the difference of CDSN between the first and last visit (Figure 4C). The same tendency was observed with CCL13, already described to be higher in AD patients and to be reduced during treatment[29] (Figure 4A-C). Interestingly, an opposite trend was observed with CXADR. After treatment some patients showed an increase of this protein that correlates strongly with an improvement in EIS scores (Figure 4C).

EIS scores on non-lesional skin correlate with the number of filaggrin repeats

FLG exon 3 is composed of 10, 11 or 12 tandem repeats. Each filaggrin repeat is 972 base pairs long, which is much longer than the fragment length in Illumina short-read sequencing. Such regions of the genome cannot be resolved by short-read sequencing due to repeat sequences. Thus, a direct quantification of *FLG* copy number is not possible. Here, we developed an alternative

This article is protected by copyright. All rights reserved

approach to quantify the normalized read coverage within the *FLG* exon 3 region. The assumption is that the reads coverage of exon 3 region is proportional to the length of exon 3, as well as to the number of tandem repeats inside. A higher read coverage represents a higher number of tandem repeats. In the following text, normalized read coverage and *FLG copy number* will be used interchangeably. We examined the correlation of estimated *FLG* copy number with EIS scores. Interestingly, in patients EIS scores measured on the non-lesional volar and dorsal forearm correlate significantly with the *FLG* copy number. Therefore, patients with lower *FLG* repeats and a likely weaker barrier function tend to have lower EIS scores, (Figure 5A and B). No correlation was observed in controls (Figure 5C and D).

In both patients and controls, pathogenic mutations in genes associated with TJs were identified. Mutations in the genes *MPP5*, *PATJ* (Protein Associated to Tight Junctions), *PRKAB1* and *FARP2* were shown to be unique for AD patients and absent in controls. Out of these four, patients carrying a mutation in *PATJ* gene, which encodes for a TJ scaffold protein, showed lower EIS scores on the volar forearm, indicating compromised skin barrier function (Figure 5E).

Accepted Article

This article is protected by copyright. All rights reserved

Accepted Article

Discussion

The present study demonstrates for the first time the ability of EIS to characterize the skin barrier function of patients with AD. The Nevisense© device utilizes EIS to assess epithelial tissues at a broad range of frequencies and at several depths, gathering a large amount of information from the tissue which is then analyzed using AI-based algorithms. Nevisense is already approved and in clinical use for the detection of melanoma in the US, EU and Australia using a similar approach. It has been validated in the world's largest melanoma detection study and described in various studies.[30, 31]

Our initial research focused on the use of this device for the detection of skin barrier defects. The method was shown to be successful in detecting skin barrier defects induced in mice by enzymes targeting barrier molecules such as papain, trypsin and cholera toxin. In addition, physical stripping of the epidermis by tape stripping showed a significant decrease in skin EIS. These results proved EIS to be an effective method to directly assess epithelial barrier defects *in vivo*.[19]

Due to the complexity of human skin compared to mouse skin and the heterogeneity of AD patients, in the present study we developed artificial intelligence-based algorithms, which we called EIS algorithms, to interpret the large amount of data in the Nevisense skin impedance measurements. After being trained to discriminate between healthy skin and lesional and non-lesional skin of AD patients, EIS algorithms calculated an EIS score in the range of 0 to 1 for each measurement, where higher scores indicate stronger skin barrier and lower scores indicate weaker skin barrier. Our data show that EIS algorithms exhibit a good diagnostic ability with relatively good specificity and sensitivity when distinguishing between skin of healthy controls and non-lesional skin of patients diagnosed with AD. They also show an even better ability to distinguish between lesional skin and non-lesional skin adjacent to a lesion. When comparing the AUCs of the respective ROC curves, EIS performs significantly better than TEWL in both comparisons.

The ability to differentiate between healthy skin of controls and non-lesional skin of AD patients indicates a potential to use EIS for the identification of atopic subjects and even for the prediction of the development of AD in infants, where an invasive tissue assessment is not recommended,or of other skin barrier-related disease exacerbations. In addition, the ability to characterize lesional and adjacent skin could potentially be useful in determining the subclinical

This article is protected by copyright. All rights reserved

spread of barrier damage. Monitoring, research and the analysis of non-lesional AD skin has been very scarce so far. Our findings suggest that with EIS it may be possible to monitor the non-lesional skin of AD patients, to assess healing response and to predict exacerbation. An increase in EIS scores on non-lesional skin towards scores typically observed on healthy skin might suggest that healing process is underway, while their decrease might suggest that an exacerbation may be developing as an early predictive biomarker, indicating the need to reinforce a treatment. Also, EIS may support the clinical decision to change the type of treatment if the scores do not indicate healing.

We observed that EIS scores correlate with several serum proteins associated with inflammatory and immune responses in AD. These proteins were upregulated in the blood of patients at the time of their hospitalization. By performing enrichment analysis using MetaCore software, we could examine the role of these proteins within molecular pathways. Interestingly, the most significantly enriched pathways were associated with the tissue migration of mast cells, eosinophils, basophils and neutrophils. Many of the significantly upregulated chemokines, such as CCL13, CCL2, CCL3, CCL7, CXCL8, as well as other molecules such as IRAK1, IRAK4 and FG2, which are involved in IL-1 signaling, show a significant inverse correlation with EIS scores, suggesting that patients with a pronounced inflammatory state seem to have a weaker barrier function. In fact, memory T lymphocytes, dendritic cell subsets, eosinophils and mast cells have already been described to take part in the pathogenesis of AD by infiltrating the perivascular, subepidermal and intraepidermal areas and several chemokines have been linked to the recruitment of these inflammatory cell subtypes to the skin in AD, including CCL2, CCL3, CCL7, CCL13, CXCL8.[32, 33] IL-1 signaling is well-known to be involved in the AD pathogenesis.[34] For some of these inflammatory markers such as CCL2 significant positive correlations between their blood level and their expression in both lesional and non-lesional skin have been reported.[35, 36] Interestingly, we observed a significant inverse correlation between CDSN and EIS scores. This protein has been associated with skin diseases such as AD, psoriasis, hypotrichosis and peeling skin syndrome, due to its importance in skin barrier function.[26, 37] In our patients CDSN is significantly upregulated in serum, probably because of the disruption of the epidermal barrier, and inversely correlates with EIS scores.

This study also suggests that EIS may have utility for objective lesion follow-up. Our data show that EIS scores increased during patients' stay at the clinic. Patients underwent several types of treatments, which were independently prescribed without any link to the present study. Within

This article is protected by copyright. All rights reserved

the same time frame, TEWL also decreased, suggesting the restoration of skin barrier. In addition, EIS scores inversely correlated with the pruritus scores and SCORAD calculated at the same visit. Furthermore, when looking at the change of inflammation- and immune response-related proteins in response to treatment, we observed that inflammatory proteins were downregulated and barrier molecules were upregulated after three weeks. In particular, CCL13 and CDSN were both downregulated and their reduction inversely correlated with the increase of EIS, whereas CXADR, a protein essential for TJs integrity and in epithelial tissues repair[27, 28], increased in patients after the therapy and this increment positively correlated with the increase in EIS. All these observations suggest that EIS can be useful for lesion follow-up to assess the improvement of the epidermal barrier following a given treatment. In addition, EIS may be useful for monitoring the skin and healing response in clinical trials to assess the effects of drugs or emollients. Furthermore, no gold standard for the assessment of disease severity in AD currently exists. Our data suggests that EIS could provide an objective measurement as an alternative or complement to current scoring systems such as SCORAD, which are based on clinical signs and subjective symptoms.

There appears to be a significant difference between lesional skin and the non-lesional skin adjacent to a lesion for both EIS and TEWL, but only EIS was able to separate between the skin of healthy controls and non-lesional skin of patients. EIS therefore, in addition to being able to distinguish between the skin of healthy controls and the non-lesional skin of patients, may be able to map the extent of barrier defects radiating out sub-clinically from visible lesions. Furthermore, EIS scores from the non-lesional skin of AD patients correlated with the number of tandem repeats in the *FLG* gene, where that number has been described to affect the quantity of *FLG* expressed in the epidermis.[38] A low *FLG* repeat number has been associated with higher AD risk and dry skin.[7, 39] Although this observation suggests there is promising potential for the use of EIS for clinical diagnosisor even early detection of AD, the authors acknowledge the likely value of a study including skin biopsies to quantify skin-related proteins within and adjacent to lesions and to correlate them to EIS measurements.

A challenge in skin barrier measurements is the effect of emollients. In our study, many different emollients were used by the patients and sometimes even a mix of several emollients. Almost 70% of the AD patients used emollients in the 12 hours preceding measurements. One of the areas of future research is to further define the effect of emollients for controls and AD

This article is protected by copyright. All rights reserved

patients. In evaluating this potential effect, we noted that most patients used emollients during the whole study and when considering individual lesion changes over time or looking at only one group (i.e. lesional, adjacent, non-lesional) we did not see a clear effect from emollients. Furthermore, although there was a large volume of impedance data per EIS measurement, there was a somewhat limited number of patients and measurements used to train EIS algorithms. This can introduce a risk for 'overfitting' the algorithms. In investigating this risk and considering that algorithms were developed to distinguish between different groups, there were still good correlations with other markers like TEWL, SCORAD, serum protein biomarkers and skin barrier-related genes. Also, the progress of lesions over time could be followed and this is a further indication that the algorithms were not significantly affected by overfitting. Regardless, as more data will be collected and added to the training data set, the authors propose to further develop these algorithms and to develop new additional ones for other body sites different than forearm, as this couldn't be developed in the present study for the limited number of patients.

In addition to the potential effect of the emollients and the risk for overfitting the algorithms, our study contains other important limitations. The lack of skin biopsies was one of them, which was due to the denied consent by almost all of the enrolled patients. We recognize that a study that includes skin biopsies from both lesional and non-lesional skin would allow the quantification of proteins and lipids in the epidermis, and therefore, lead to a better characterization of the skin barrier in patients. Alternatively, tape stripping could be considered for studying skin composition. Another significant limitation was represented by the number of patients involved. Despite the large volume of impedance data per EIS measurement, the number of patients used to train and validate the EIS algorithms was low. Therefore, a more extensive study needs to be performed in the future, which will help classify patients according to their skin type, clinical phenotypes and endotypes. A larger number of patients will also allow a classification based on systemic and topical treatments to study how the different treatments affect skin barrier and, therefore, EIS measurements. Furthermore, given that our study was performed only in Caucasians, it will be good to target other ethnicities in the future studies to confirm the efficacy of EIS in other ethnic groups.

Overall, our data indicate EIS has the potential to be a reliable tool to determine in vivo skin barrier dysfunction in AD patients, providing objective help for the clinical assessment of the severity and progression of AD, a better follow-up of barrier healing and improved treatment

This article is protected by copyright. All rights reserved

Accepted Article

management, allowing the evaluation of the therapy efficacy. Ourdata also suggest that EIS may be a promising tool for the early prediction of ADdevelopment in babies, which needs to be confirmed by further research. Additionally, EIS measurements might help evaluate skin integrity after exposure to toxic substances or in other skin diseases such as toxic epidermal necrolysis, psoriasis and alopecia. Skin breakdown might also be monitored by EIS after cuts, tears, blisters or burns, or even in case of severe pressure ulcers.

An EIS measurement can be performed in a standard clinical environmentwithout the need for a climate or lighting-controlled room or for the acclimatization of the patient prior to the measurement procedure, both of which are examples of limitations of alternative methods such as TEWL or Raman Spectroscopy.[20, 21]A predeveloped algorithm can rapidly classify EIS measurement as a single value between 0 and 1, giving an easy-to-read result that allows follow-ups and comparisons. Moreover, given that AD can be classified into various clinical phenotypes, based on severity, onset, atopy, morphology, lesion localization, as well as on the association to concomitant other atopic disorders, and that some of these phenotypes are strongly associated with an altered expression of proteins important in the skin barrier, EIS might be helpful to identify these phenotypes and thereby assess the nature of the pathology.[12, 41] In conclusion, this study shows that EIS can become an important tool to assess the skin barrier in research and shows potential as a practical clinical tool for identifying a weakened or defective barrier.

This article is protected by copyright. All rights reserved

Accepted Article

References

1. Asher, M.I. *et al.* Worldwide time trends in the prevalence of symptoms of asthma, allergic rhinoconjunctivitis, and eczema in childhood: ISAAC Phases One and Three repeat multicountry cross-sectional surveys. *Lancet***368**,733-743 (2006).
2. Eichenfield, L.F. *et al.* Guidelines of care for the management of atopic dermatitis: section 1. Diagnosis and assessment of atopic dermatitis. *J Am Acad Dermatol***70**,338-351 (2014).
3. Drucker, A.M. *et al.*The Burden of Atopic Dermatitis: Summary of a Report for the National Eczema Association. *J Invest Dermatol***137**,26-30 (2017).
4. Agrawal, R. & Woodfolk, J.A. Skin barrier defects in atopic dermatitis. *Curr Allergy Asthma Rep***14**,433 (2014).
5. Altunbulakli, C. *et al.* Relations between epidermal barrier dysregulation and Staphylococcus species-dominated microbiome dysbiosis in patients with atopic dermatitis. *J Allergy Clin Immunol***142**,1643-1647 e1612 (2018).
6. Cabanillas, B. & Novak, N. Atopic dermatitis and filaggrin. *Curr Opin Immunol***42**,1-8 (2016).
7. Brown, S.J. *et al.* Intragenic copy number variation within filaggrin contributes to the risk of atopic dermatitis with a dose-dependent effect. *J Invest Dermatol***132**,98-104 (2012).
8. De Benedetto, A. *et al.* Tight junction defects in patients with atopic dermatitis. *J Allergy Clin Immunol***127**,773-786 e771-777 (2011).
9. Thijs, J. *et al.* Biomarkers for atopic dermatitis: a systematic review and meta-analysis. *Curr Opin Allergy Clin Immunol***15**,453-460 (2015).
10. Thijs, J.L., de Bruin-Weller, M.S. & Hijnen, D. Current and Future Biomarkers in Atopic Dermatitis. *Immunol Allergy Clin North Am***37**,51-61 (2017).
11. Pugliarello, S., Cozzi, A., Gisondi, P. & Girolomoni, G. Phenotypes of atopic dermatitis. *J Dtsch Dermatol Ges***9**,12-20 (2011).
12. Czarnowicki, T., He, H., Krueger, J.G. & Guttman-Yassky, E. Atopic dermatitis endotypes and implications for targeted therapeutics. *J Allergy Clin Immunol***143**,1-11 (2019).
13. Kelleher, M. *et al.* Skin barrier dysfunction measured by transepidermal water loss at 2 days and 2 months predates and predicts atopic dermatitis at 1 year. *J Allergy Clin Immunol***135**,930-935 e931 (2015).

This article is protected by copyright. All rights reserved

14. Kelleher, M.M. *et al.*Skin barrier impairment at birth predicts food allergy at 2 years of age. *J Allergy Clin Immunol***137**,1111-1116 e1118 (2016).
15. Horimukai, K. *et al.* Application of moisturizer to neonates prevents development of atopic dermatitis. *J Allergy Clin Immunol***134**,824-830 e826 (2014).
16. Simpson, E.L. *et al.* Emollient enhancement of the skin barrier from birth offers effective atopic dermatitis prevention. *J Allergy Clin Immunol***134**,818-823 (2014).
17. Goleva, E., Berdyshev, E. & Leung, D.Y. Epithelial barrier repair and prevention of allergy. *J Clin Invest***129**,1463-1474 (2019).
18. Leung, D.Y.M. *et al.* The nonlesional skin surface distinguishes atopic dermatitis with food allergy as a unique endotype. *Sci Transl Med***11** (2019).
19. Rinaldi, A.O. *et al.* Direct assessment of skin epithelial barrier by electrical impedance spectroscopy. *Allergy***74**,1934-1944 (2019).
20. Berardesca, E., Loden, M., Serup, J., Masson, P. & Rodrigues, L.M. The revised EEMCO guidance for the in vivo measurement of water in the skin. *Skin Res Technol***24**,351-358 (2018).
21. Eberhardt, K., Stiebing, C., Matthaus, C., Schmitt, M. & Popp, J. Advantages and limitations of Raman spectroscopy for molecular diagnostics: an update. *Expert Rev Mol Diagn***15**,773-787 (2015).
22. Akdeniz, M., Gabriel, S., Lichterfeld-Kottner, A., Blume-Peytavi, U. & Kottner, J. Transepidermal water loss in healthy adults: a systematic review and meta-analysis update. *Br J Dermatol***179**,1049-1055 (2018).
23. DePristo, M.A. *et al.* A framework for variation discovery and genotyping using next-generation DNA sequencing data. *Nat Genet***43**,491-498 (2011).
24. Langmead, B. & Salzberg, S.L. Fast gapped-read alignment with Bowtie 2. *Nat Methods***9**,357-359 (2012).
25. Magi, A., Tattini, L., Pippucci, T., Torricelli, F. & Benelli, M. Read count approach for DNA copy number variants detection. *Bioinformatics***28**,470-478 (2012).
26. Oji, V. *et al.* Loss of corneodesmosin leads to severe skin barrier defect, pruritus, and atopy: unraveling the peeling skin disease. *Am J Hum Genet***87**,274-281 (2010).
27. Cohen, C.J. *et al.* The coxsackievirus and adenovirus receptor is a transmembrane component of the tight junction. *Proc Natl Acad Sci U S A***98**,15191-15196 (2001).

This article is protected by copyright. All rights reserved

Accepted Article

28. Luissint, A.C., Lutz, P.G., Calderwood, D.A., Couraud, P.O. & Bourdoulous, S. JAM-L-mediated leukocyte adhesion to endothelial cells is regulated in cis by alpha4beta1 integrin activation. *J Cell Biol***183**,1159-1173 (2008).
29. Brunner, P.M. *et al.* Author Correction: The atopic dermatitis blood signature is characterized by increases in inflammatory and cardiovascular risk proteins. *Sci Rep***8**,8439 (2018).
30. Malvehy, J. *et al.* Clinical performance of the Nevisense system in cutaneous melanoma detection: an international, multicentre, prospective and blinded clinical trial on efficacy and safety. *Br J Dermatol***171**,1099-1107 (2014).
31. Svoboda, R.M., Prado, G., Mirsky, R.S. & Rigel, D.S. Assessment of clinician accuracy for diagnosing melanoma on the basis of electrical impedance spectroscopy score plus morphology versus lesion morphology alone. *J Am Acad Dermatol***80**,285-287 (2019).
32. Nedoszytko, B., Sokolowska-Wojdylo, M., Ruckemann-Dziurdzinska, K., Roszkiewicz, J. & Nowicki, R.J. Chemokines and cytokines network in the pathogenesis of the inflammatory skin diseases: atopic dermatitis, psoriasis and skin mastocytosis. *Postepy Dermatol Alergol***31**,84-91 (2014).
33. Pivarcsi, A. & Homey, B. Chemokine networks in atopic dermatitis: traffic signals of disease. *Curr Allergy Asthma Rep***5**,284-290 (2005).
34. Jensen, L.E. Targeting the IL-1 family members in skin inflammation. *Curr Opin Invest Dr***11**,1211-1220 (2010).
35. Brunner, P.M. *et al.* The atopic dermatitis blood signature is characterized by increases in inflammatory and cardiovascular risk proteins. *Sci Rep***7**,8707 (2017).
36. Brunner, P.M. *et al.* The blood proteomic signature of early-onset pediatric atopic dermatitis shows systemic inflammation and is distinct from adult long-standing disease. *J Am Acad Dermatol***81**,510-519 (2019).
37. Allen, M. *et al.* Corneodesmosin expression in psoriasis vulgaris differs from normal skin and other inflammatory skin disorders. *Lab Invest***81**,969-976 (2001).
38. Romero, V., Hosomichi, K., Nakaoka, H., Shibata, H. & Inoue, I. Structure and evolution of the filaggrin gene repeated region in primates. *BMC Evol Biol***17**,10 (2017).
39. Ginger, R.S., Blachford, S., Rowland, J., Rowson, M. & Harding, C.R. Filaggrin repeat number polymorphism is associated with a dry skin phenotype. *Arch Dermatol Res***297**,235-241 (2005).

This article is protected by copyright. All rights reserved

40. Clausen, M.L., Slotved, H.C., Krogfelt, K.A. & Agner, T. Tape Stripping Technique for Stratum Corneum Protein Analysis. *Sci Rep***6**,19918 (2016).
41. Bieber, T. *et al.* Clinical phenotypes and endophenotypes of atopic dermatitis: Where are we, and where should we go? *J Allergy Clin Immunol***139**,S58-S64 (2017).

Accepted Article

This article is protected by copyright. All rights reserved

Accepted Article

Demographics	Patients with AD (n=36)	Control group without AD (n=28)
Age (years) ± SD	45.82 ± 14.75	39.45 ± 9.97
Female	69 %	65 %
Male	31 %	35 %
Ethnicity (Caucasian)	100 %	100 %
Family history of atopy	80 %	50 %
Family history of AD	58 %	15 %
Asthma	67 %	5 %
Food allergy	73 %	0 %
Allergic rhinitis	82 %	30 %
Disease onset (year) ± SD	6 ± 9.39	-
SCORAD at visit 1 ± SD	43,93 ± 19.20	-

Table 1: Demographic characteristics of the study subjects.

This article is protected by copyright. All rights reserved

Accepted Article

Figure legends

Figure 1: **EIS can differentiate between the skin of healthy subjects and the lesional or non-lesional skin of AD patients.** Artificial intelligence-based algorithms calculated an EIS score (where 0 represents a defective barrier and 1 a healthy barrier) for each measurement (**a**) on the volar forearm (Non-lesionalalgorithm, see "Materials and methods") and (**b**) on the dorsal forearm (Lesionalalgorithm, see "Materials and methods"). Measurements shown in B were performed both on a lesion and on a non-lesional area close to that lesion (referred to as an "adjacent" site). TEWL was measured in healthy controls and AD patients on the same body sites. TEWL is expressed in g/m^2h. **: $p<0.01$, ***: $p<0.001$, ****: $p<0.0001$. Medians of triplicates are shown. (**c**) A ROC curve was generated from measurements on the non-lesional volar forearm of AD patients and healthy controls. In the box at the bottom right corner of each ROC curve, the AUC (Area Under the Curve) values are shown. These values can be between 0 and 1; the higher the AUC is, the better the algorithm is at distinguishing between two different conditions.

Figure 2:**Significantly upregulated inflammation- and immune response-related proteins correlate with EIS scores.** (**a**) Volcano plot of the differential expression of proteins measured in serum by proteomic Olink (Uppsala, Sweden) multiplex assay is shown. Comparing AD patients and controls, the statistically significantly ($p<0.05$) different proteins are marked in red. (**b**) The difference in the expression of the top 9 most significantly upregulated proteins in AD and control groups is shown in the dot plots. ****: $p<0.0001$, ***: $p<0.001$. (**c**) Pathways enriched with upregulated proteins using MetaCore are shown. For each protein, heatmaps show the $\log_2$ fold change calculated from the comparison between AD patients and healthy controls. (**d**) The inverse correlations of some of the most significantly upregulated proteins with EIS scores on non-lesional skin of AD patients and controls are shown; (**e**) the matrix illustrates the level of significance of the spearman coefficients for all the significant inverse correlations between lesional and non-lesional forearm EIS scores and significantly upregulated serum proteins. The proteins are listed in order of the level of statistically significant difference between AD patients and controls, while the stars in each box show the significance of each correlation. In both d and e, EIS scores and normalized protein expressions at visit 1 and visit 3 are included. *<0,05, **: $p<0.01$, ***: $p<0.001$, ****: $p<0.0001$

This article is protected by copyright. All rights reserved

Accepted Article

Figure 3: **Lesion healing in response to treatment correlated with an increase in EIS scores and a decrease in TEWL.** EIS (**a**) and TEWL (**b**) were measured in AD patients on a lesion on the dorsal forearm over a time of 21 days, which corresponds to the duration of the treatment at the clinic. "First visit" and "Last visit" correspond to the measurements made at admission and at the end of the treatment respectively. EIS scores were calculated by an artificial intelligence model (Follow-upalgorithm, see "Material and Methods"). TEWL is expressed in g/m^2h. **: $p<0.01$. Medians of triplicates are shown. (**c**) EIS scores inversely correlated at both first and last visit with TEWL. (**d**) The correlation between the difference in EIS scores from first to last visit and the difference of pruritus score (normalized to 0-1 range) from first to last visit is shown. (**e-f**) EIS scores on lesional dorsal forearm at first and last visit inversely correlates with pruritus scores (**e**) and SCORAD (**f**) at the same visits.

Figure 4:**The change in EIS score during the 21-day treatment correlates with the correction of proinflammatory proteins in the direction of healthy controls.** (**a**) Volcano plot of the differential expression of proteins measured in serum at first and last visit by proteomic Olink (Uppsala, Sweden) multiplex assay is shown. The statisticallysignificantly ($p<0.05$) changed proteins between AD patients and controls are marked in red. (**b**) The different expression of CDSN, CCL13 and CXADR significantly changed in AD patients between first and last visit is shown in the dot plots. *<0,05, **: $p<0.01$, ****: $p<0.0001$. (**c**) The correlation between the difference in EIS scores on forearm from first to last visit and the difference in CDSN, CCL13 and CXADR (values normalized to 0-1 range) from first to last visit is shown.

Figure 5: **EIS scores on non-lesional skin correlate with the number of filaggrin repeats.** EIS scores on non-lesional volar (**a**) and dorsal (**b**) forearm positively correlates with FLG copy number in patients, but not in controls in the same body sites (**c-d**). (**e**) Comparing TJs-related genes between controls and AD, PATJ, MPP5, FARB2 and PRKAB1 genes presented mutation only in AD. Patients were separated in two groups, with or without mutations. EIS scores from non-lesional volar forearm are shown. ***: $p<0.001$.

This article is protected by copyright. All rights reserved

Accepted Article

Supplementary Materials

Supplementary materials and methods

Supplementary figure 1:**No effect seen from recent emollient use on EIS score.**Patients were divided in two groups, with emollients and without (w/o) emollients, according to their use of emollients withinthe 12 hours prior to the measurements. For each group, EIS scores on the volar forearm (Non lesional algorithm, see "Materials and methods") are shown.

Supplementary figure 2: **EIS is better than TEWL in characterizing lesional and adjacent non-lesional skin of AD patients.**ROC curves were generated(**a**) from measurements on adjacent non-lesional dorsal forearm of AD patients and healthy controls, (**b**) from measurements on lesional dorsal forearm and adjacent non-lesional dorsal forearm of AD patients and (**c**) from measurements on the lesional dorsal forearm of AD patients and on the dorsal forearm of controls. All triplicate measurements were used. In the box at the bottom right corner of each ROC curve, the AUC (Area Under the Curve) values are shown. These values can be between 0 and 1; the higher the AUC is, the better the algorithm is at distinguishing between two different conditions.

Supplementary figure 3: **Heatmaps with differences in upregulated inflammation- and immune response-related proteinsbetween AD patients and control subjects.** For each pathway enriched with upregulated proteins using MetaCore, heatmaps show the difference in the protein relative expressions between AD patients and control subjects.

Supplementary figure 4:**Machine learning algorithm development workflow.**

This article is protected by copyright. All rights reserved

Supplementary table 1: **List of proteins significantly up- or downregulated in patients compared to controls.** Differentially expressed proteins measured in serum by proteomic Olink (Uppsala, Sweden) multiplex assay are listed. Comparing AD patients and controls, log_2 fold change and relative p-values are shown for each of the significantly changed proteins.

Supplementary table2: **List of all significant correlations between EIS scores and significantly upregulated serum proteins.** Spearman coefficients and p-values of the inverse correlations between the significantly upregulated serum proteins and EIS scores on dorsal lesional forearm (Lesional skin), dorsal non-lesional forearm adjacent to the lesion (Adjacent) and on non lesional volar forearm (Non lesional) are listed.

Supplementary table 3:**List of EIS scores and TEWL values on lesional forearm, SCORAD and pruritus scores**. For each of the patients shown in figure 3A and 3B, EIS scores, TEWL values, SCORAD and pruritus scores calculated at the time of their hospitalization (First visit) and at the end of the 3-week treatment (Last visit) are reported.

Supplementary table 4: **List of proteins significantly up- or downregulated in patients comparing last visit to first visit.** Differentially expressed proteins measured in serum by proteomic Olink (Uppsala, Sweden) multiplex assay are listed. Comparing first and last visit in AD, log_2 fold change and relative p-values are shown for each of the significantly changed proteins.

Supplementary table 5: **Number of patients and controls included in each figure.** For each figure in this paper, the table shows the EIS algorithm used, the body site, the visits included and the total number of patients and controls.

This article is protected by copyright. All rights reserved

all_14842_f1-5.pdf

Accepted Article

Electrical impedance spectroscopy for the characterization of skin barrier in atopic dermatitis

Short title**:** A new tool for skin barrier assessment in AD

Arturo O. Rinaldi[1,], Angelica Korsfeldt[2], Siobhan Ward[1,3], Daniel Burla[1], Anita Dreher[3], Marja Gautschi[4], Britta Stolpe[4], Ge Tan[1,5], Eugen Bersuch[3], David Melin[2], Nima Askary Lord[2], Simon Grant[2], Per Svedenhag[2], Kristina Tsekova[4], Peter Schmid-Grendelmeier[3,6], Matthias Möhrenschlager[4], Ellen D. Renner[4,7], Cezmi A. Akdis[1,3*]

Affiliations

1 Swiss Institute of Allergy and Asthma Research (SIAF), Davos, Switzerland

2 SciBase AB, Sundbyberg, Sweden

3 Christine Kühne – Center for Allergy Research and Education (CK-CARE), Davos, Switzerland

4 Hochgebirgsklinik - High Altitude Clinic (HGK), Davos, Switzerland

5 Functional Genomics Center Zurich, ETH Zurich/University of Zurich, Zurich, Switzerland

6 Department of Dermatology, University Hospital, Zurich

7 Environmental Medicine - UNIKA-T, Technical University, Munich and Helmholtz Center

Corresponding author

Cezmi A. Akdis, Swiss Institute of Allergy and Asthma Research (SIAF), Herman Burchard Strasse 9, CH-7265, Davos, Tel +41814100841, Email akdisac@siaf.uzh.ch

This article is protected by copyright. All rights reserved

Accepted Article

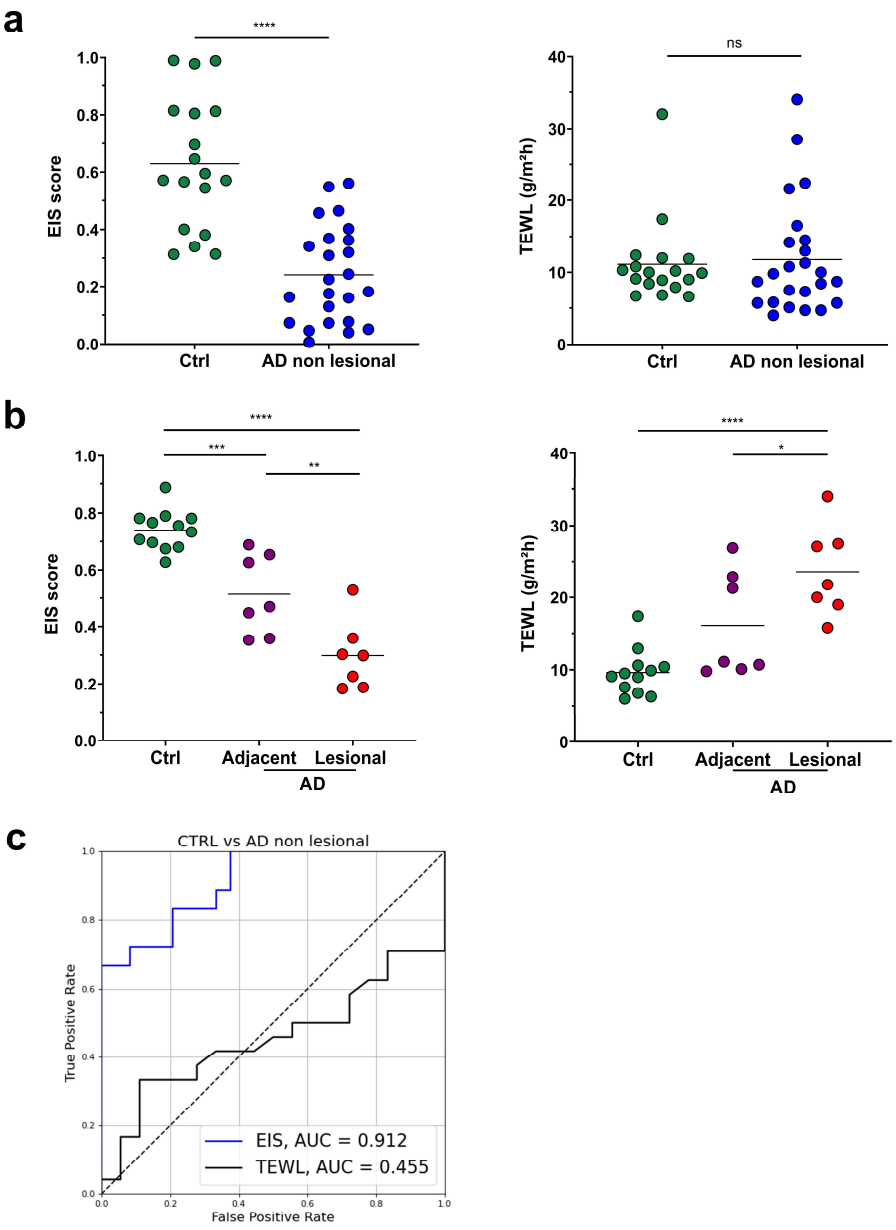
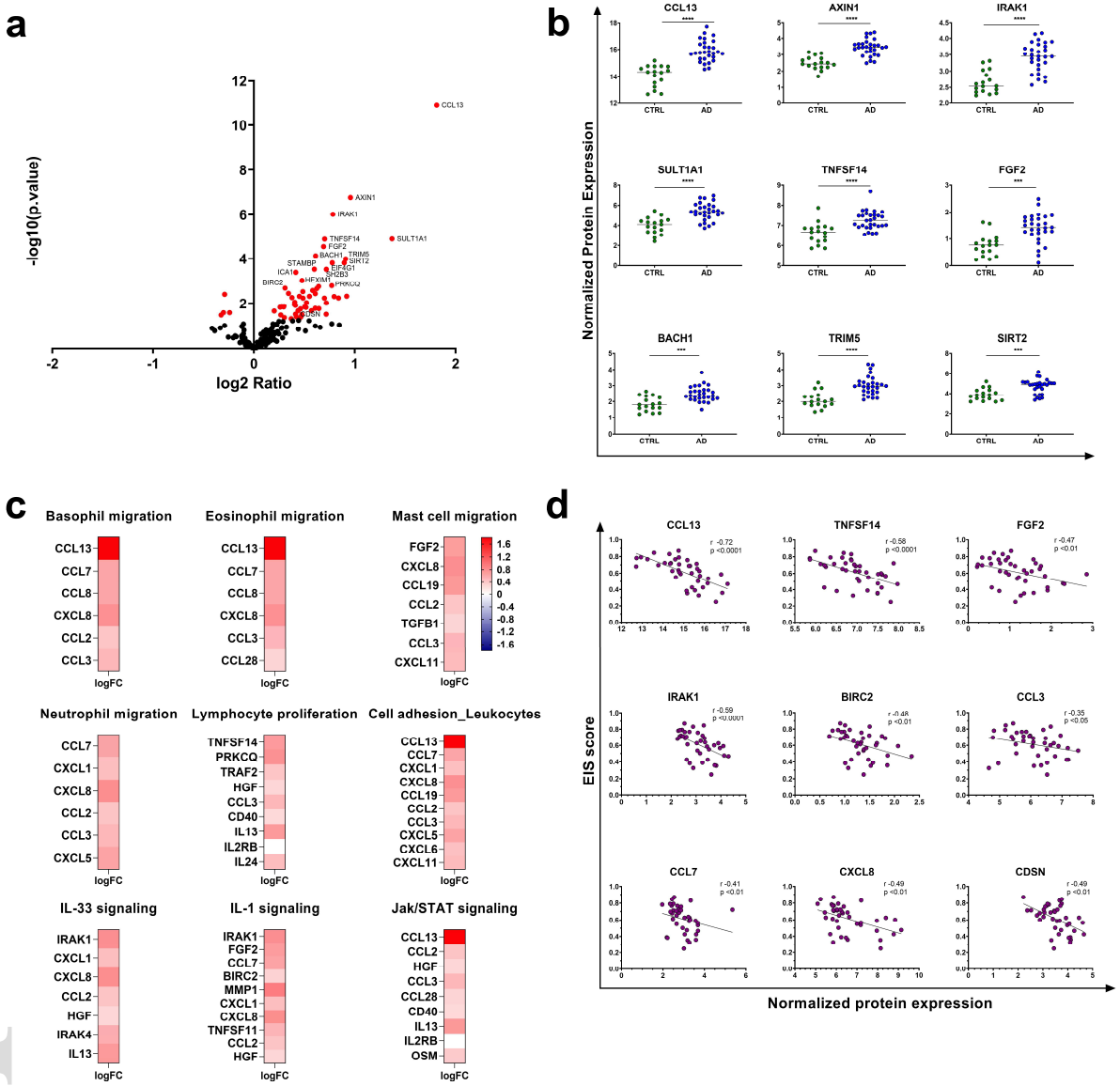


Figure 1: **EIS can differentiate between the skin of healthy subjects and the lesional or non-lesional skin of AD patients.** Artificial intelligence-based algorithms calculated an EIS score (where 0 represents a defective barrier and 1 a healthy barrier) for each measurement (**a**) on the volar forearm (Non-lesional algorithm, see "Materials and methods") and (**b**) on the dorsal forearm (Lesional algorithm, see "Materials and methods"). Measurements shown in B were performed both on a lesion and on a non-lesional area close to that lesion (referred to as an "adjacent" site). TEWL was measured in healthy controls and AD patients on the same body sites. TEWL is expressed in g/m^2h. **: $p<0.01$, ***: $p<0.001$, ****: $p<0.0001$. Medians of triplicates are shown. (**c**) A ROC curve was generated from measurements on the non-lesional volar forearm of AD patients and healthy controls. In the box at the bottom right corner of each ROC curve, the AUC (Area Under the Curve) values are shown. These values can be between 0 and 1; the higher the AUC is, the better the algorithm is at distinguishing between two different conditions.

This article is protected by copyright. All rights reserved

Accepted Article



This article is protected by copyright. All rights reserved

Accepted Article

Figure 2: **Significantly upregulated inflammation- and immune response-related proteins correlate with EIS scores.** (**a**) Volcano plot of the differential expression of proteins measured in serum by proteomic Olink (Uppsala, Sweden) multiplex assay is shown. Comparing AD patients and controls, the statistically significantly ($p<0.05$) different proteins are marked in red. (**b**) The difference in the expression of the top 9 most significantly upregulated proteins in AD and control groups is shown in the dot plots. ****: $p<0.0001$, ***: $p<0.001$. (**c**) Pathways enriched with upregulated proteins using MetaCore are shown. For each protein, heatmaps show the $\log_2$ fold change calculated from the comparison between AD patients and healthy controls. (**d**) The inverse correlations of some of the most significantly upregulated proteins with EIS scores on non-lesional skin of AD patients and controls are shown; (**e**) the matrix illustrates the level of significance of the spearman coefficients for all the significant inverse correlations between lesional and non-lesional forearm EIS scores and significantly upregulated serum proteins. The proteins are listed in order of the level of statistically significant difference between AD patients and controls, while the stars in each box show the significance of each correlation. In both d and e, EIS scores and normalized protein expressions at visit 1 and visit 3 are included. *<0,05, **: $p<0.01$, ***: $p<0.001$, ****: $p<0.0001$

This article is protected by copyright. All rights reserved

Accepted Article

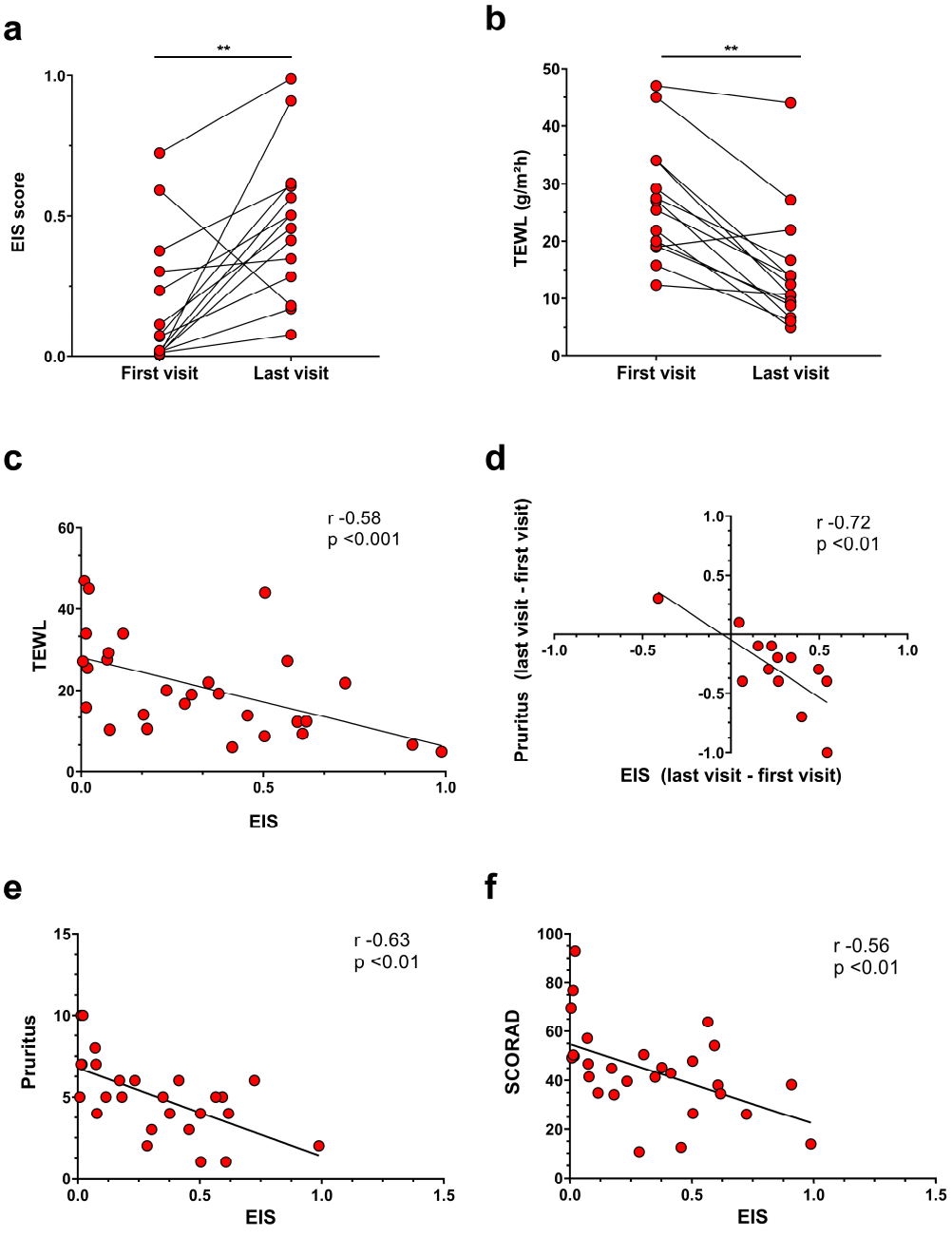


Figure 3: **Lesion healing in response to treatment correlated with an increase in EIS scores and a decrease in TEWL.** EIS (**a**) and TEWL (**b**) were measured in AD patients on a lesion on the dorsal forearm over a time of 21 days, which corresponds to the duration of the treatment at the clinic. "First visit" and "Last visit" correspond to the measurements made at admission and at the end of the treatment respectively. EIS scores were calculated by an artificial intelligence model (Follow-up algorithm, see "Material and Methods"). TEWL is expressed in g/m^2h. **: $p<0.01$. Medians of triplicates are shown. (**c**) EIS scores inversely correlated at both first and last visit with TEWL. (**d**) The correlation between the difference in EIS scores from first to last visit and the difference of pruritus score (normalized to 0-1 range) from first to last visit is shown. (**e-f**) EIS scores on lesional dorsal forearm at first and last visit inversely correlates with pruritus scores (**e**) and SCORAD (**f**) at the same visits.

This article is protected by copyright. All rights reserved

Accepted Article

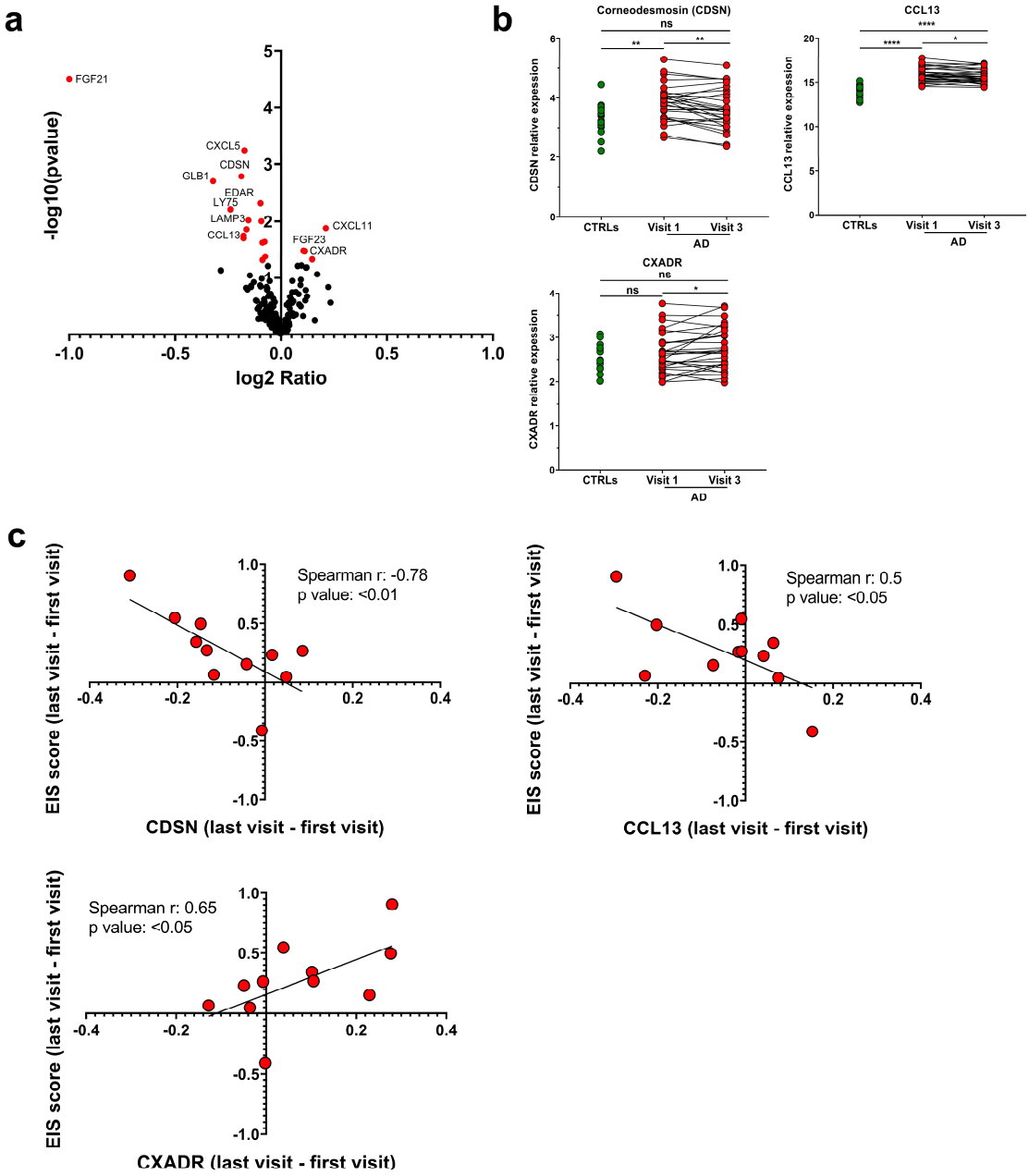


Figure 4: **The change in EIS score during the 21-day treatment correlates with the correction of proinflammatory proteins in the direction of healthy controls.** (**a**) Volcano plot of the differential expression of proteins measured in serum at first and last visit by proteomic Olink (Uppsala, Sweden) multiplex assay is shown. The statistically significantly ($p<0.05$) changed proteins between AD patients and controls are marked in red. (**b**) The different expression of CDSN, CCL13 and CXADR significantly changed in AD patients between first and last visit is shown in the dot plots. *<0,05, **: $p<0.01$, ****: $p<0.0001$. (**c**) The correlation between the difference in EIS scores on forearm from first to last visit and the difference in CDSN, CCL13 and CXADR (values normalized to 0-1 range) from first to last visit is shown.

This article is protected by copyright. All rights reserved

Accepted Article

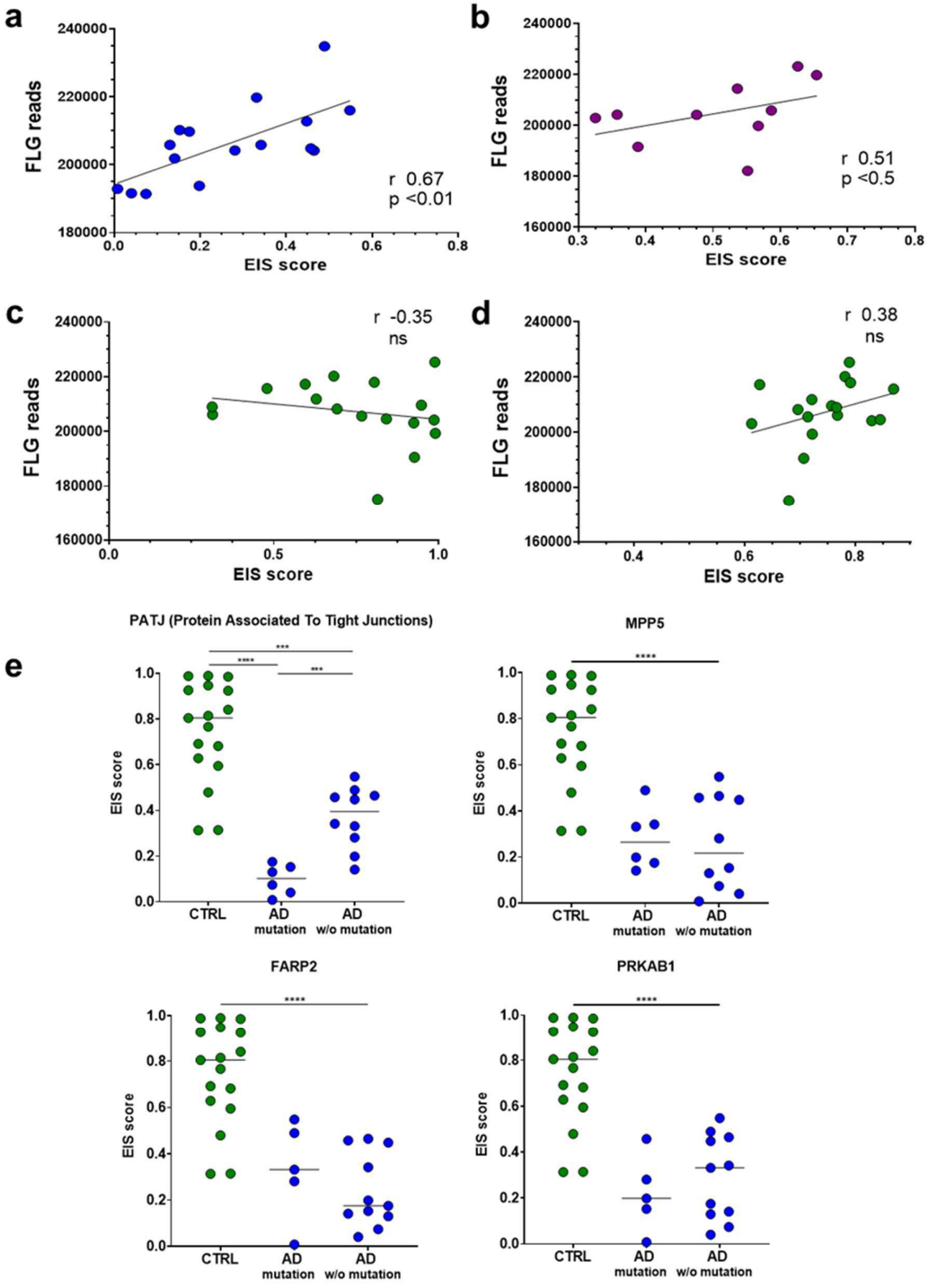


Figure 5: **EIS scores on non-lesional skin correlate with the number of filaggrin repeats.** EIS scores on non-lesional volar (**a**) and dorsal (**b**) forearm positively correlates with FLG copy number in patients, but not in controls in the same body sites (**c-d**). (**e**) Comparing TJs-related genes between controls and AD, PATJ, MPP5, FARB2 and PRKAB1 genes presented mutation only in AD. Patients were separated in two groups, with or without mutations. EIS scores from non-lesional volar forearm are shown. ***: p<0.001.

This article is protected by copyright. All rights reserved

Electrical impedance spectroscopy for the characterization of skin barrier in atopic dermatitis

Short title**:** A new tool for skin barrier assessment in AD

Arturo O. Rinaldi[1,], Angelica Korsfeldt[2], Siobhan Ward[1,3], Daniel Burla[1], Anita Dreher[3], Marja Gautschi[4], Britta Stolpe[4], Ge Tan[1,5], Eugen Bersuch[3], David Melin[2], Nima Askary Lord[2], Simon Grant[2], Per Svedenhag[2], Kristina Tsekova[4], Peter Schmid-Grendelmeier[3,6], Matthias Möhrenschlager[4], Ellen D. Renner[4,7], Cezmi A. Akdis[1,3*]

Affiliations

1 Swiss Institute of Allergy and Asthma Research (SIAF), Davos, Switzerland

2 SciBase AB, Sundbyberg, Sweden

3 Christine Kühne – Center for Allergy Research and Education (CK-CARE), Davos, Switzerland

4 Hochgebirgsklinik - High Altitude Clinic (HGK), Davos, Switzerland

5 Functional Genomics Center Zurich, ETH Zurich/University of Zurich, Zurich, Switzerland

6 Department of Dermatology, University Hospital, Zurich

7 Environmental Medicine - UNIKA-T, Technical University, Munich and Helmholtz Center

Corresponding author

Cezmi A. Akdis, Swiss Institute of Allergy and Asthma Research (SIAF), Herman Burchard Strasse 9, CH-7265, Davos, Tel +41814100841, Email akdisac@siaf.uzh.ch

Supplementary Material

Supplementary Materials and methods

Training of EIS algorithms

Subjects with and or without AD were randomly separated into two groups: one group (55-65% of the subjects) for the training of the neural network and one group for the validation of the obtained algorithm. Three different algorithms (otherwise known as neural network 'models') were trained as follows:

- **Non-lesional algorithm**

  Non-lesional measurements from all visits were included. Triplicate measurements from 56 visits were used for training and triplicate measurements from 42 visits were used for validation where the median value of the triplicates was used in the graphs.

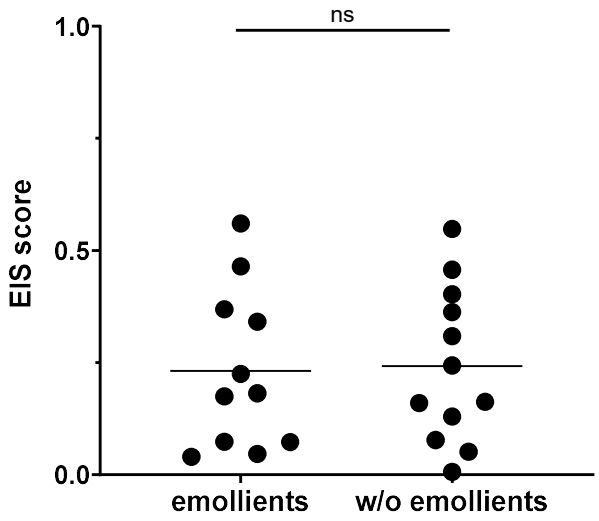
- **Lesional algorithm**

  Measurements on dorsal forearm from visit 1 were included. Since the purpose of this algorithm was to assess the lesional skin and the unaffected skin adjacent to the lesion before the start of treatments, other visits were not included in the training. Triplicate measurements from 42 visits were used for training and triplicate measurements from 30 visits were used for validation.

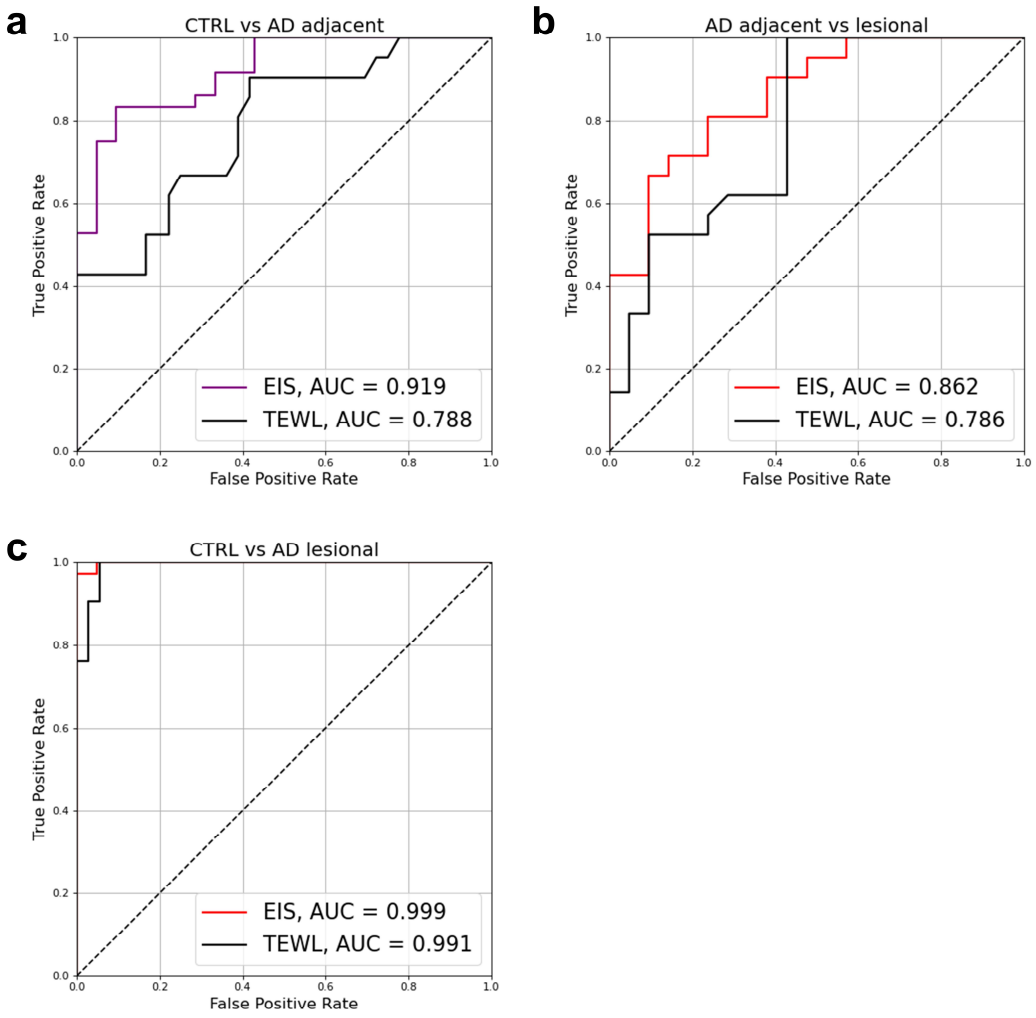
- **Follow-up algorithm**

  Measurements on both dorsal forearm and volar forearm from all visits were included. 172 triplicate measurements were used for training and 97 triplicate measurements for validation.

Measurements were always done in triplicates. The coefficient of variation in healthy controls was 2.93%.

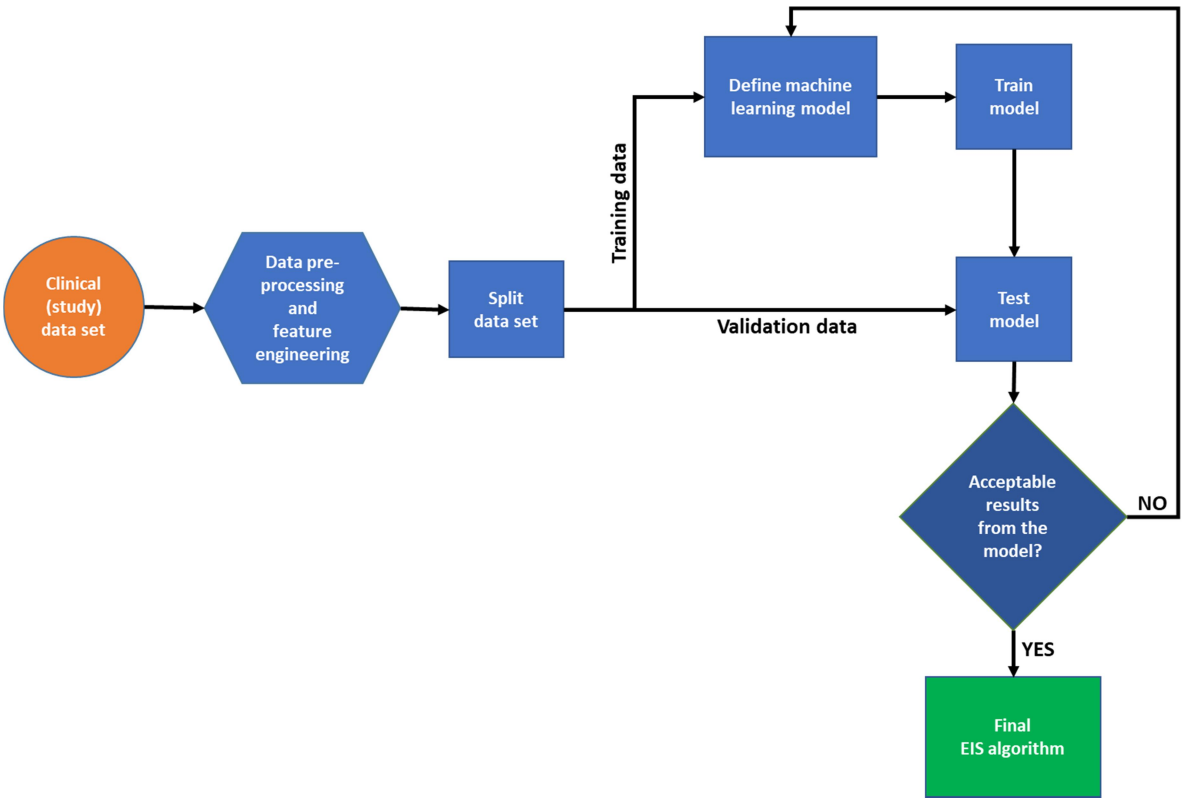


Supplementary figure 1: **No effect seen from recent emollient use on EIS score.** Patients were divided in two groups, with emollients and without (w/o) emollients, according to their use of emollients within the 12 hours prior to the measurements. For each group, EIS scores on the volar forearm (Non lesional algorithm, see “Materials and methods”) are shown.



Supplementary figure 2: **EIS is better than TEWL in characterizing lesional and adjacent non-lesional skin of AD patients.** ROC curves were generated (**a**) from measurements on adjacent non-lesional dorsal forearm of AD patients and healthy controls, (**b**) from measurements on lesional dorsal forearm and adjacent non-lesional dorsal forearm of AD patients and (**c**) from measurements on the lesional dorsal forearm of AD patients and on the dorsal forearm of controls. All triplicate measurements were used. In the box at the bottom right corner of each ROC curve, the AUC (Area Under the Curve) values are shown. These values can be between 0 and 1; the higher the AUC is, the better the algorithm is at distinguishing between two different conditions.

Supplementary figure 3: **Heatmaps with differences in upregulated inflammation- and immune response-related proteins between AD patients and control subjects.** For each pathway enriched with upregulated proteins using MetaCore, heatmaps show the difference in the protein relative expressions between AD patients and control subjects.



Supplementary figure 4: **Machine learning algorithm development workflow.**

Protein name	p value	log Fold Change
CCL13	1.28E-11	1.81
AXIN1	1.81E-07	0.96
IRAK1	9.72E-07	0.78
SULT1A1	1.27E-05	1.37
TNFSF14	1.30E-05	0.70
FGF2	2.83E-05	0.69
BACH1	7.43E-05	0.61
TRIM5	1.03E-04	0.91
SIRT2	1.53E-04	0.90
EIF4G1	1.54E-04	0.78
STAMBP	2.91E-04	0.60
SH2B3	2.96E-04	0.72
ICA1	4.01E-04	0.42
HEXIM1	9.12E-04	0.48
PRKCQ	0.0015	0.77
CCL7	0.0017	0.64
BIRC2	0.0020	0.31
CCL8	0.0021	0.62
SRPK2	0.0026	0.58
PPP1R9B	0.0029	0.48
BTN3A2	0.0035	0.34
HCLS1	0.0036	0.61
CNTNAP2	0.0038	-0.29
MMP1	0.0047	0.92
CXCL1	0.0047	0.45
CLEC7A	0.0047	0.55
CXCL8	0.0048	0.79
CLEC6A	0.0054	0.38
PLXNA4	0.0056	0.84
DFFA	0.0057	0.49
MGMT	0.0057	0.70
TRAF2	0.0087	0.40
TNFSF11	0.0092	0.52
CCL19	0.0094	0.72
IRF9	0.0112	0.40
CCL2	0.0122	0.41
TGFB1	0.0133	0.30
HGF	0.0134	0.27
CCL3	0.0143	0.50
CCL28	0.0145	0.29
CD40	0.0148	0.26
CLEC4D	0.0152	0.52
PRDX5	0.0165	0.61
CXCL5	0.0172	0.64
EGLN1	0.0177	0.46
CXCL6	0.0215	0.44
IRAK4	0.0216	0.57
CKAP4	0.0220	0.20
LAG3	0.0261	-0.30
FGF5	0.0263	-0.24
IL13	0.0306	0.72
CDSN	0.0306	0.41
CXCL11	0.0319	0.48
TREM1	0.0332	0.27
IL2RB	0.0336	-0.32
IL24	0.0389	0.47
ITGA6	0.0404	0.42
PIK3AP1	0.0436	0.46
AREG	0.0437	0.30
OSM	0.0490	0.37

Supplementary table 1: **List of proteins significantly up- or downregulated in patients compared to controls.** Differentially expressed proteins measured in serum by proteomic Olink (Uppsala, Sweden) multiplex assay are listed. Comparing AD patients and controls, $\log_2$ fold change and relative p-values are shown for each of the significantly changed

Protein name	Lesional skin		Adjacent		Non lesional	
	Spearman coefficient	p value	Spearman coefficient	p value	Spearman coefficient	p value
CCL13	-0.79	1.74E-09	-0.72	6.33E-08	-0.57	3.90E-06
AXIN1	-0.61	2.50E-05	-0.61	1.72E-05	-0.68	7.45E-09
IRAK1	-0.62	2.10E-05	-0.59	3.55E-05	-0.64	1.31E-07
SULT1A1	-0.62	2.02E-05	-0.51	0.0006	-0.54	1.73E-05
TNFSF14	-0.58	7.41E-05	-0.58	5.35E-05	-0.51	5.11E-05
FGF2	-0.54	3.72E-04	-0.47	0.0017	-0.57	3.63E-06
BACH1	-0.59	5.29E-05	-0.60	2.30E-05	-0.48	0.0002
TRIM5	-0.68	1.31E-06	-0.60	3.03E-05	-0.62	3.01E-07
SIRT2	-0.59	6.53E-05	-0.44	0.0033	-0.53	2.31E-05
EIF4G1	-0.60	3.66E-05	-0.49	0.0009	-0.54	2.06E-05
STAMBP	-0.57	0.0001	-0.48	0.0011	-0.52	3.64E-05
SH2B3	-0.42	0.0064	-0.40	0.0091	-0.52	4.58E-05
ICA1	-0.47	0.0023	-0.48	0.0012	-0.45	0.0005
HEXIM1	-0.51	0.0007	-0.47	0.0017	-0.55	1.01E-05
PRKCQ	-0.52	0.0006	-0.37	0.0156	-0.52	4.80E-05
CCL7	-0.41	0.0091	-0.41	0.0075	-0.36	0.0067
BIRC2	-0.52	0.0006	-0.48	0.0012	-0.51	5.29E-05
SRPK2	-0.51	0.0008	-0.51	0.0006	-0.35	0.0079
PPP1R9B	-0.47	0.0025	-0.45	0.0031	-0.46	0.0003
HCLS1	-0.49	0.0015	-0.49	0.0009	-0.32	0.0164
CXCL8	-0.54	0.0003	-0.49	0.0011	-0.54	1.69E-05
CLEC6A	-0.37	0.0175	-0.47	0.0019	-0.44	0.0008
DFFA	-0.61	0.0000	-0.52	0.0004	-0.47	0.0003
MGMT	-0.37	0.0192	-0.34	0.0256	-0.30	0.0255
TRAF2	-0.52	0.0006	-0.39	0.0101	-0.39	0.0030
IRF9	-0.43	0.0056	-0.24	0.1231	-0.41	0.0017
CCL2	-0.38	0.0147	-0.23	0.1366	-0.28	0.0353
HGF	-0.48	0.0018	-0.49	0.0010	-0.46	0.0004
CCL3	-0.44	0.0048	-0.35	0.0233	-0.58	2.47E-06
CLEC4D	-0.39	0.0130	-0.41	0.0067	-0.49	0.0001
PRDX5	-0.44	0.0046	-0.36	0.0192	-0.42	0.0012
EGLN1	-0.45	0.0035	-0.47	0.0015	-0.31	0.0220
IRAK4	-0.43	0.0052	-0.39	0.0107	-0.36	0.0058
CKAP4	-0.50	0.0011	-0.61	1.87E-05	-0.35	0.0082
CDSN	-0.37	0.0176	-0.49	0.0011	-0.21	0.1148

Supplementary table 2: **List of all significant correlations between EIS scores and significantly upregulated serum proteins.** Spearman coefficients and p-values of the inverse correlations between the significantly upregulated serum proteins and EIS scores on dorsal lesional forearm (Lesional skin), dorsal non-lesional forearm adjacent to the lesion (Adjacent) and on non lesional volar forearm (Non lesional) are listed.

	EIS scores		TEWL		SCORAD		Pruritus score	
	First visit	Last visit	First visit	Last visit	First visit	Last visit	First visit	Last visit
Patient_1	0.115	0.456	34.00	13.80	34.90	12.50	5	3
Patient_2	0.724	0.988	21.80	5.00	26.20	13.90	6	2
Patient_3	0.303	0.349	19.00	21.90	50.50	41.30	3	5
Patient_4	0.018	0.171	25.40	14.00	49.90	44.90	7	6
Patient_5	0.013	0.078	34.00	10.40	76.80	41.42	10	4
Patient_6	0.005	0.909	27.10	6.70	69.60	38.20	NA	NA
Patient_7	0.593	0.181	12.30	10.60	54.20	34.14	5	5
Patient_8	0.071	0.284	27.50	16.70	57.10	10.70	8	2
Patient_9	0.377	0.607	19.20	9.40	45.20	38.00	4	1
Patient_10	0.234	0.503	20.00	8.80	39.60	47.88	6	4
Patient_11	0.009	0.505	47.00	44.00	49.24	26.54	5	1
Patient_12	0.014	0.414	15.80	6.10	50.38	42.94	7	6
Patient_13	0.021	0.566	45.00	27.20	92.90	63.84	10	5
Patient_14	0.075	0.618	29.20	12.40	46.78	34.58	7	4

Supplementary table 3: **List of EIS scores and TEWL values on lesional forearm, SCORAD and pruritus scores**. For each of the patients shown in figure 3A and 3B, EIS scores, TEWL values, SCORAD and pruritus scores calculated at the time of their hospitalization (First visit) and at the end of the 3-week treatment (Last visit) are reported.

68

69

70

71

Protein name	p value	log Fold Change
FGF21	3.16E-05	-1.00
CXCL5	5.72E-04	-0.17
CDSN	0.0016	-0.19
GLB1	0.0020	-0.32
LY75	0.0049	-0.10
EDAR	0.0062	-0.24
LAMP3	0.0096	-0.15
MASP1	0.0100	-0.09
CXCL11	0.0133	0.21
HNMT	0.0139	-0.16
SH2D1A	0.0180	-0.18
CCL13	0.0202	-0.18
TPSAB1	0.0234	-0.08
ITGB6	0.0242	-0.09
CXADR	0.0335	0.11
FGF23	0.0340	0.11
ITGA6	0.0427	-0.07
MMP1	0.0480	0.15
PTH1R	0.0492	-0.09

Supplementary table 4: **List of proteins significantly up- or downregulated in patients comparing last visit to first visit.** Differentially expressed proteins measured in serum by proteomic Olink (Uppsala, Sweden) multiplex assay are listed. Comparing first and last visit in AD, $\log_2$ fold change and relative p-values are shown for each of the significantly changed proteins.

Figure	EIS algorithm	Body site	Number of subjects in figure				Comment
			CTRL	AD			
				Non-lesional	Non-lesional adjacent	lesional	
1a	Non-lesional	Volar forearm	18	24	-	-	*Only validation data are shown. All visits are included.*
1b	Lesional	Dorsal forearm	12	-	7	7	*Only validation data are shown. Only visit 1 (before treatment) is included.*
1c	Non-lesional	Volar forearm	18	24	-	-	*Only validation data are shown. All visits are included.*
2a	NA	NA	*NA*	*NA*	*NA*	*NA*	
2b	NA	NA	*NA*	*NA*	*NA*	*NA*	*17 controls and 29 AD subjects, normalized protein expression from Olink. Only visit 1 (before treatment) is included.*
2c	NA	NA	*NA*	*NA*	*NA*	*NA*	
2d	Lesional	Dorsal forearm	17	-	23	-	*Only subjects with blood sample and AD subjects with adjacent measurements on dorsal forearm. Visit 1 and 3 (first and last visits) are included.*
2e	NA	NA	*NA*	*NA*	*NA*	*NA*	
3a	Follow-up	Dorsal forearm	-	-	-	28	*Only AD subjects with lesions on dorsal forearm and measurements for first and last visit. Visit 1 and 3 (first and last visits) are included.*
3b	NA	Dorsal forearm	-	-	-	28	*Only AD subjects with lesions on dorsal forearm and measurements for first and last visit. Visit 1 and 3 (first and last visits) are included.*
3c	Follow-up	Dorsal forearm	-	-	-	28	*Only AD subjects with lesions on dorsal forearm and measurements for first and last visit. Visit 1 and 3 (first and last visits) are included.*
3d	Follow-up	Dorsal forearm	-	-	-	13	*Only AD subjects with lesions on dorsal forearm, score for pruritus and measurements for first and last visit. Visit 1 and 3 (first and last visits) are included.*
3e	Follow-up	Dorsal forearm	-	-	-	26	*Only AD subjects with lesions on dorsal forearm, score for pruritus and measurements for first and last visit. Visit 1 and 3 (first and last visits) are included.*
3f	Follow-up	Dorsal forearm	-	-	-	26	*Only AD subjects with lesions on dorsal forearm, SCORAD and measurements for first and last visit. Visit 1 and 3 (first and last visits) are included.*
4a	NA	NA	*NA*	*NA*	*NA*	*NA*	
4b	NA	NA	*NA*	*NA*	*NA*	*NA*	*17 controls and 29 AD subjects, normalized protein expression from Olink. Visit 1 and 3 (first and last visits) are included.*
4c	Follow-up	Dorsal forearm	-	-	-	11	*Only AD subjects with lesions on dorsal forearm and with blood samples. Visit 1 and 3 (first and last visits) are included.*
5a	Non-lesional	Volar forearm	-	16	-	-	*Only AD subjects with non-lesional antecubital area and blood sample.*
5b	Lesional	Dorsal forearm	-	-	10	-	*Only AD subjects with non-lesional dorsal measurement and blood sample.*
5c	Non-lesional	Volar forearm	17	-	-	-	
5d	Lesional	Dorsal forearm	17	-	-	-	
5e	Non-lesional	Volar forearm	17	16	-	-	*Only AD subjects with non-lesional antecubital area and blood sample.*
S1	Non-lesional	Volar forearm	-	23	-	-	*Only patients with information about the use emollients are included. All visits are included.*
S2a	Lesional	Dorsal forearm	12	-	7	-	*Only validation data are shown. Only visit 1 (before treatment) is included.*
S2b	Lesional	Dorsal forearm	-	-	7	7	*Only validation data are shown. Only visit 1 (before treatment) is included.*
S2c	Lesional	Dorsal forearm	12	-	-	7	*Only validation data are shown. Only visit 1 (before treatment) is included.*
S3	NA	NA	*NA*	*NA*	*NA*	*NA*	*17 controls and 29 AD subjects*
S4	NA	NA	*NA*	*NA*	*NA*	*NA*	

Supplementary table 5: **Number of patients and controls included in each figure.** For each figure in this paper (S stands for supplementary figure), the table shows the EIS algorithm used, the body site, the visits included and the total number of patients and controls.